SUPPLEMENTARY MATERIAL OF IEEE TCST PAPER

Amritam Das*[1], Martijn Princen[1], Mahnaz Shokpour Roudbari[2], Amol Khalate[2], Siep Weiland[1]

Abstract

The supplementary material contains three items: a) an academic example of the digital twin; b) the proof of Algorithm IV.1; c) the proof of theorem VI.1.

Index Terms

Inkjet Printing, Thermo-Fluidic Processes, Spatially Interconnected Systems, Soft Sensing, Optimal Control.

NOMENCLATURE

$\bar{h}$	average convective heat transfer $W/(m^{2\circ}C)$
$\dot{Q}_r$	Radiation Heat transfer W
ϵ	Emissivity $-$
μ	Viscosity Ns/m^2
ρ	Density Kg/m^3
k	Thermal conductivity$W/(m \cdot^\circ C)$
A_i	Surface area m^2
A_{cross}	Cross-sectional aream^2
A_{i-j}	Contact area m^2
c_i	Specific heat capacity $J/(kg^\circ C)$
D_h	Hydraulic diameter m
F_{ij}	View factor between surfaces $-$
h	Heat transfer coefficient $W/(m^{2\circ}C)$
H_v	Convective heat transfer coefficient $W/^\circ C$
H_d	Conductive heat transfer coefficient $W/^\circ C$
l_i	Length from center of mass to surface m
L_c	Characteristic length$m$
m_i	Mass kg
P_{cross}	Perimeter of the cross-section$m$
R	Thermal resistance $^\circ C/W$
T_i	Temperature $^\circ C$
v	velocity m/s
Bi	Biot Number$-$
Nu	Nusselt number $-$
Re	Reynolds Number $-$

[1]Eindhoven University of Technology, Department of Electrical Engineering, Control Systems group, P.O. Box 513, 5600 MB Eindhoven, The Netherlands. E-mail: am.das@tue.nl, M_princen@hotmail.com, s.weiland@tue.nl

[2]Canon Production Printing B.V., Van der Grintenstraat 10, 5914 HH Venlo, The Netherlands. E-mail: mahnaz.shokrpour@cpp.canon, amolkhalate@gmail.com

*Corresponding author: Amritam Das. Tel. +31(0)402472300.

I. Academic Example of Digital Twin

Figure 1 presents a simplified example to demonstrate the use of the graph-theoretic modeling approach.

(a) Cross-sectional Schemtics

(b) Graph Structure

Fig. 1: Example of a thermo-fluidic process

Here, the liquid tank $L1$ has a time-varying inflow of $Q_{in}(t)$ m^3/s and outflow of $Q_r(t)$ m^3/s. Every individual nozzle $Ln1$, $Ln2$, $Ln3$ has liquid outflow with a time-varying flow rate $Q_{ni}(t)$ m^3/s, $i \in \{1,2,3\}$.

A. Graph $\mathcal{G}$

There are six nodes; $\mathcal{N} := \{\mathcal{N}_{S1}, \mathcal{N}_{S2}, \mathcal{N}_{L1}, \mathcal{N}_{Ln1}, \mathcal{N}_{Ln2}, \mathcal{N}_{Ln3}\}$.

B. Topology

The adjacent matrix $A \in \mathbb{R}^{6\times 6}$ is defined as follows

$$A = \begin{bmatrix} 0 & 1 & 1 & 0 & 0 & 0 \\ 1 & 0 & 1 & 1 & 1 & 1 \\ 1 & 1 & 0 & 0 & 0 & 0 \\ 0 & 1 & 1 & 0 & 0 & 0 \\ 0 & 1 & 1 & 0 & 0 & 0 \\ 0 & 1 & 1 & 0 & 0 & 0 \end{bmatrix} \tag{1}$$

It is evident that the topology of Lni is identical for $i = \{1,2,3\}$. In other words, topologically, there is no difference in the interconnection between any of the three nozzles and the rest of the graph. This is a major advantage for building graph-theoretic model.

C. Node dynamics

The equations governing the thermo-fluidic processes consist of three kinds of thermal energy transfer. They are:

1) *Conduction*: Heat transfer within solid nodes or via contact between solid nodes.
2) *Convection*: Heat transfer between the solid and liquid nodes.
3) *Advection*: Heat transfer via bulk movement of the liquid from one channel to the other.

In the following items, the thermo-fluidic processes are derived per node:

$\mathcal{N}_{S1}$: Its temperature T_{S1} ($^\circ C$) is influenced by convection with $\mathcal{N}_{L1}$ and conduction with $\mathcal{N}_{S1}$ according to the following equation of energy conservation

$$C_{S1}\frac{dT_{S1}}{dt} = H_{d,1}(T_{S2} - T_{S1}) + H_{v,1}(T_{L1} - T_{S1}).$$

Substituting the expressions of $H_{d,1}, H_{v,1}$, one obtains

$$\underbrace{m_{S1}c_{S1}\frac{dT_{S1}}{dt}}_{Thermal\ storage} = \underbrace{\frac{1}{R_{tot}}}_{Conduction}(T_{S2} - T_{S1}) + \underbrace{\frac{Nu_{L1}\cdot k_{L1}}{D_{hL1}}A_{S1-L1}(T_{L1} - T_{S1})}_{Convection}. \tag{2}$$

Here, the equivalent thermal resistance is $R_{tot} = \frac{l_{S1}}{A_{S1-S2}k_{S1}} + \frac{l_g}{A_{S1-S2}k_g} + \frac{l_{S2}}{A_{S1-S2}k_{S2}}$.

$\mathcal{N}_{L1}$: Its temperature T_{L1} ($^\circ C$) is influenced by advection and convection according to the following equation of energy conservation

$$C_{L1}\frac{dT_{L1}}{dt} = H_{v,1}(T_{S1} - T_{L1}) + H_{v,2}(T_{S2} - T_{L1}) + H_{a,1}(t)(T_{in} - T_{L1}).$$

In other words,

$$\underbrace{m_{L1}c_{L1}\frac{dT_{L1}}{dt}}_{Thermal\ storage} = \underbrace{\frac{Nu_{L1}\cdot k_{L1}}{D_{hL1}}A_{S1-L1}}_{Convection}(T_{S1}-T_{L1}) + \underbrace{\frac{Nu_{L1}\cdot k_{L1}}{D_{hL1}}A_{S2-L1}}_{Convection}(T_{S2}-T_{L1})$$
$$+ \underbrace{\rho_{in}c_{in}(Q_r(t)+\sum_{i=1}^{3}Q_{ni}(t)}_{Advection}(T_{in}-T_{L1})). \tag{3}$$

$\mathcal{N}_{Lni}$: For individual liquid nozzle $\mathcal{N}_{Lni}$ $i\in\{1,2,3\}$, the governing equation is identical. Hence, as an example, the governing equation of temperature T_{Lni} ($°C$) for node $\mathcal{N}_{Lni}$ is

$$C_{Lni}\frac{dT_{Lni}}{dt} = H_{v,ni}(T_{S2}-T_{Lni}) + H_{a,ni}(t)(T_{L1}-T_{Lni}).$$

$$\underbrace{m_{Lni}c_{Lni}\frac{dT_{Lni}}{dt}}_{Thermal\ storage} = \underbrace{\frac{Nu_{Lni}\cdot k_{Lni}}{D_{hLni}}A_{S2-Lni}}_{Convection}(T_{S2}-T_{Lni}) + \underbrace{\rho_{L1}c_{L1}Q_{ni}(t)}_{Advection}(T_{L1}-T_{Lni}). \tag{4}$$

To obtain the thermo-fluidic model of every individual nozzle, one simply has to repeat (4) by substituting the physical parameters with index $i\in\{1,2,3\}$.

$\mathcal{N}_{S2}$: This node is connected with all of the other nodes. Similar to $\mathcal{N}_{S1}$, it temperature, T_{S2} ($°C$), is governed by the following equation of energy conservation:

$$C_{S2}\frac{dT_{S2}}{dt} = H_{d,1}(T_{S1}-T_{S2}) + H_{v,2}(T_{L1}-T_{S2}) + \sum_{i=1}^{3}H_{v,ni}(T_{Lni}-T_{S2})$$

$$\underbrace{m_{S2}c_{S2}\frac{dT_{S2}}{dt}}_{Thermal\ storage} = \underbrace{\frac{1}{R_{tot}}}_{Conduction}(T_{S1}-T_{S2}) + \underbrace{\frac{Nu_{L1}\cdot k_{L1}}{D_{hL1}}A_{S2-L1}}_{Convection}(T_{L1}-T_{S2}) + \sum_{i=1}^{3}\underbrace{\frac{Nu_{Lni}\cdot k_{Lni}}{D_{hLni}}A_{S2-Lni}}_{Convection}(T_{Lni}-T_{S2}) \tag{5}$$

Remark I.1. By construction, modularity is a key attribute in the thermo-fluidic process. As the dynamics and topological interconnection of every individual nozzle is identical with respect to the entire graph, the digital twin simply requires repetition of identical models based on the number of nozzles. This is a crucial advantage of graph-theoretic framework in building digital twin.

D. *State-space representation of a node*

For example, for $\mathcal{N}_{S1}$, the temperature evolution can be re-written in the following state-space form:

$$\begin{bmatrix}\dot{T}_{S1}\\ w_{S1,S2}\\ w_{S1,L1}\\ q_{S1}\end{bmatrix} = \begin{bmatrix}\frac{(H_{d,1}+H_{v,1})}{C_{S1}} & \frac{H_{d,1}}{C_{S1}} & \frac{H_{v,1}}{C_{S1}} & 1 & 0\\ 1 & 0 & 0 & 0 & 0\\ 1 & 0 & 0 & 0 & 0\\ 0 & 0 & 0 & 0 & 0\end{bmatrix}\begin{bmatrix}T_{S1}\\ v_{S1,S2}\\ v_{S1,L1}\\ p_{S1}\end{bmatrix},\ \begin{bmatrix}v_{S1,S2}\\ v_{S1,L1}\end{bmatrix} = \begin{bmatrix}0 & 0 & 1 & 0\\ 0 & 0 & 0 & 1\end{bmatrix}\begin{bmatrix}w_{S1,S2}\\ w_{S1,L1}\\ w_{S2,S1}\\ w_{L1,S1}\end{bmatrix}, p_{S1}=q_{S1}. \tag{6}$$

E. *Interconnection Structure*

The interconnection relation $v=\bar{M}w$ is given below.

$$\underbrace{\begin{bmatrix}v_{S1,S2}\\ v_{S1,L1}\\ v_{S2,S1}\\ v_{S2,L1}\\ v_{S2,Ln1}\\ v_{L1,S_1}\\ v_{L1,S2}\\ v_{Lni,S2}\\ v_{Lni,L1}\end{bmatrix}}_{v} = \underbrace{\begin{bmatrix}0&0&1&0&0&0&0&0&0\\ 0&0&0&0&0&1&0&0&0\\ 1&0&0&0&0&0&0&0&0\\ 0&0&0&0&0&0&1&0&0\\ 0&0&0&0&0&0&0&0&1\\ 0&1&0&0&0&0&0&0&0\\ 0&0&0&1&0&0&0&0&0\\ 0&0&0&0&1&0&0&0&0\\ 0&0&0&0&0&0&0&1&0\end{bmatrix}}_{\bar{M}}\underbrace{\begin{bmatrix}w_{S1,S2}\\ w_{S1,L1}\\ w_{S2,S1}\\ w_{S2,L1}\\ w_{S2,Ln1}\\ w_{L1,S1}\\ w_{L1,S2}\\ w_{L1,Lni}\\ w_{Lni,S2}\end{bmatrix}}_{w} \tag{7}$$

For brevity, only one nozzle, $\mathcal{N}_{Lni}$, is considered and it can be repeated for $i\in\{1,2,3\}$. This is again a major advantage for building the digital twin. Irrespective of the number of nozzles, as they have identical dynamics and identical topology, up-scaling the model is a straightforward task.

F. Determining the representation $\mathcal{P}_{\mathrm{I}}$

Now one can easily build the representation $\mathcal{P}_{\mathrm{I}}$ by stacking all the signals:

$$\begin{bmatrix}\dot{T}_{S1}(t)\\ \dot{T}_{S2}(t)\\ \dot{T}_{L1}(t)\\ \dot{T}_{Lni}(t)\end{bmatrix} = \underbrace{\begin{bmatrix} -\frac{(H_{d,1}+H_{v,1})}{C_{S1}} & 0 & 0 & 0\\ 0 & -\frac{H_{d,1}+H_{v,2}+H_{v,n1}}{C_{S2}} & 0 & 0\\ 0 & 0 & -\frac{H_{v,1}+H_{v,2}}{C_{L1}} & 0\\ 0 & 0 & 0 & -\frac{H_{v,ni}}{C_{Lni}}\end{bmatrix}}_{A_{xx}} \begin{bmatrix}T_{S1}(t)\\ T_{S2}(t)\\ T_{L1}(t)\\ T_{Lni}(t)\end{bmatrix} + \underbrace{\begin{bmatrix}1&0&0&0\\0&1&0&0\\0&0&1&0\\0&0&0&1\end{bmatrix}}_{B_{xp}} p(t)$$

$$+ \underbrace{\begin{bmatrix} \frac{H_{d,1}}{C_{S1}} & \frac{H_{v,1}}{C_{S1}} & 0 & 0 & 0 & 0 & 0 & 0 & 0 & 0 & 0\\ 0 & 0 & \frac{H_{d,1}}{C_{S2}} & \frac{H_{v,2}}{C_{S2}} & \frac{H_{v,n1}}{C_{S2}} & \frac{1}{C_{S2}} & 0 & 0 & 0 & 0 & 0\\ 0 & 0 & 0 & 0 & 0 & 0 & \frac{H_{v,1}}{C_{L1}} & \frac{H_{v,2}}{C_{L1}} & 0 & 0 & 0\\ 0 & 0 & 0 & 0 & 0 & 0 & 0 & 0 & \frac{H_{v,ni}}{C_{Lni}} & 0 & \frac{1}{C_{Lni}}\end{bmatrix}}_{B_{xv}} v(t), \tag{8}$$

$$q(t) = \underbrace{\begin{bmatrix}0&0&0&0\\0&0&0&0\\0&0&-\frac{\rho_{L1}c_{L1}}{C_{L1}}&0\\0&0&0&-\frac{\rho_{L1}c_{L1}}{C_{Lni}}\end{bmatrix}}_{C_{qx}} \begin{bmatrix}T_{S1}(t)\\ T_{S2}(t)\\ T_{L1}(t)\\ T_{Lni}(t)\end{bmatrix} + \underbrace{\begin{bmatrix}0&0&0&0&0&0&0&0&0&0&0\\0&0&0&0&0&0&0&0&0&0&0\\0&0&0&0&0&0&0&0&0&0&0\\0&0&0&0&0&0&0&0&0&\frac{\rho_{L1}c_{L1}}{C_{Lni}}&0\end{bmatrix}}_{D_{qv}} v(t), \tag{9}$$

$$w(t) = \underbrace{\begin{bmatrix}1&0&0&0\\1&0&0&0\\0&1&0&0\\0&1&0&0\\0&1&0&0\\0&0&1&0\\0&0&1&0\\0&0&1&0\\0&0&0&1\\0&0&0&0\\0&0&0&0\end{bmatrix}}_{C_{wx}} \begin{bmatrix}T_{S1}(t)\\ T_{S2}(t)\\ T_{L1}(t)\\ T_{Lni}(t)\end{bmatrix}, \tag{10}$$

$$y(t) = \underbrace{\begin{bmatrix}0&0&0&1\end{bmatrix}}_{C_{yx}} \begin{bmatrix}T_{S1}(t)\\ T_{S2}(t)\\ T_{L1}(t)\\ T_{Lni}(t)\end{bmatrix}, \tag{11}$$

$$p(t) = \underbrace{\begin{bmatrix}1&0&0&0\\0&1&0&0\\0&0&Q_r(t)+\sum_{i=1}^{3} Q_{ni}(t)&0\\0&0&0&Q_{ni}(t)\end{bmatrix}}_{\bar{\Theta}(t)} q(t). \tag{12}$$

The other equivalent representation $\mathcal{P}_{\mathrm{II}}$, or $\mathcal{P}_{\mathrm{III}}$ can be derived by eliminating signals (v, w) or (p, q).

II. Proof of Algorithm IV.1

Proof: Consider a class of stable, second-order, single-input-single-output systems that has the following representation:

$$\begin{aligned} z(n+1) =& A_s z(n) + B_s w(n), \\ y(n) =& C_s z(n). \end{aligned} \tag{13}$$

Here, for $n \in \mathbb{N} \cup \{0\}$, $z(n) \in \mathbb{R}^2$ is a vector with two internal states and $w(n) \in \mathbb{R}$ is the applied impulsive input. The output signal $y(n) \in \mathbb{R}$ is modeled as (14).

$$y(n) = \alpha e^{-\zeta n T_s} \sin(\omega n T_s + \phi) + \gamma; \qquad n \in \mathbb{N}. \tag{14}$$

A. Step 1: Determining the poles

The first task is to find an estimate of the state matrix $A_s \in \mathbb{R}^{2\times 2}$. To this end, the Hankel matrix is constructed using the data $\{s_n, n \in \mathbb{N}_{[1,N]}\}$ as follows:

$$H = \begin{bmatrix} s_1 & \dots & s_{L-1} & s_L \\ s_2 & \dots. & s_L & s_{L+2} \\ \vdots & \ddots & \vdots & \vdots \\ s_{N-L} & \dots. & s_{N-2} & s_{N-1} \\ s_{N-L+1} & \dots & s_{N-1} & s_N \end{bmatrix} = \mathcal{O}_{N-L+1}\mathcal{R}_L,$$

where, the observability matrix $\mathcal{O}_{N-L+1}$ and the reachability matrix $\mathcal{R}_L$ are defined as

$$\mathcal{R}_L := \begin{bmatrix} B_s & A_s B_s & \cdots & A_s^{L-1} B_s \end{bmatrix}, \mathcal{O}_{N-L+1} := \begin{bmatrix} C_s \\ C_s A_s \\ \vdots \\ C_s A_s^{N-L} \end{bmatrix}.$$

Remark II.1. (shift property of observability matrix)

$$\mathcal{O}^1_{N-L+1} A_s = \mathcal{O}^2_{N-L+1},$$

where, $\mathcal{O}^1_{N-L+1} = \begin{bmatrix} C_s \\ C_s A_s \\ \vdots \\ C_s A_s^{N-L-1} \end{bmatrix}$ and $\mathcal{O}^2_{N-L+1} = \begin{bmatrix} C_s A_s \\ \vdots \\ C_s A_s^{N-L} \end{bmatrix}$.

As, we are interested in a second order system, let the optimal 2-rank approximation of the Hankel H be given by

$$H \approx U \Sigma V^{\mathrm{H}}, \quad \Sigma := \mathrm{diag}(\sigma_1, \sigma_2), \quad \sigma_1, \sigma_2 > 0.$$

In other words,

$$H \approx \underbrace{U \Sigma^{\frac{1}{2}}}_{\mathcal{O}_{N-L+1}} \underbrace{\Sigma^{\frac{1}{2}} V^{\mathrm{H}}}_{\mathcal{R}_L}.$$

Now, using the shift property we obtain:

$$\tilde{A}_s = \Sigma^{-\frac{1}{2}} {U^1}^{\dagger} U^2 \Sigma^{\frac{1}{2}},$$

where $\tilde{A}_s = T^{-1} A_s T$ for an unknown matrix T. As the poles of the system does not change of under similarity transformation, the two poles of A_s are found by solving the eigen value ρ_k and right eigen vector v_k, $k = 1, 2$:

$$(\tilde{A}_s - \rho_k) v_k = 0$$

B. Determine ω and ζ

Using the system poles, we find the frequency ω and the damping ζ as follows:

- Natural Frequency: $\omega = \mathrm{Im}(\ln \rho_k), k = 1$ or 2.
- Damping : $\zeta = \mathrm{Re}(\ln \rho_k), k = 1$ or 2.

C. Determine α, ϕ, and γ

The amplitude α, the phase ϕ and the shift γ are found by reconstructing the signal s_n using computed values of ω, ζ. In particular:

$$\begin{aligned} y(n) &= \alpha e^{-\zeta n T_s}\sin(\omega n T_s+\phi)+\gamma = (a+jb)e^{j(\omega+j\zeta)nT_s}+(a+jb)^{*}e^{-j(\omega-j\zeta)nT_s}+\gamma. \\ &= a\Big(e^{j(\omega+j\zeta)nT_s}+e^{-j(\omega-j\zeta)nT_s}\Big)+jb\Big(e^{j(\omega+j\zeta)nT_s}-e^{-j(\omega-j\zeta)nT_s}\Big)+\gamma. \end{aligned} \tag{15}$$

Here, $a=\frac{\alpha}{2}\sin\phi$ and $a=\frac{\alpha}{2}\cos\phi$ are the unknowns coefficients and γ is the unknown offset. Using the data at samples $\{0,\cdots,N-1\}$, the unknowns can be found by solving the following linear equations:

$$\mathbf{s}=\mathbf{\Gamma}\mathbf{x}, \tag{16}$$

Here, the unknowns are $\mathbf{x} := \mathrm{col}(a,b,\gamma)$, $\mathbf{s} := \mathrm{col}(s_1,\cdots,s_N)$ is the data. Moreover the matrix is defined as $\mathbf{\Gamma} := \mathrm{col}\Big(\big[(e^{j(\omega+j\zeta)nT_s}+e^{-j(\omega-j\zeta)nT_s}) \quad j(e^{j(\omega+j\zeta)nT_s}-e^{-j(\omega-j\zeta)nT_s}) \quad 1\big]\Big)_{n\in\mathbb{N}_{[1,N]}}$ depends on ω and ζ, and . An unbiased minimum variance solution of (16), $\hat{\mathbf{x}} := \mathrm{col}(\hat{a},\hat{b},\hat{\gamma})$, accepts the following analytic expression:

$$\hat{\mathbf{x}}=(\mathbf{\Gamma}^{\mathrm{H}}\mathbf{\Gamma})^{-1}\mathbf{\Gamma}^{\mathrm{H}}\mathbf{s}. \tag{17}$$

Using computed $\hat{\mathbf{x}}$, the amplitude (α) and phase (ϕ) of the signal (14) are computed as follows:

- Amplitude: $\alpha = 2\sqrt{\mathrm{Re}(\hat{a}+j\hat{b})^2+\mathrm{Im}(\hat{a}+j\hat{b})^2}$.
- Phase : $\phi=\mathrm{Im}(\ln(\hat{a}+j\hat{b}))$.
- Offset : $\gamma=\hat{\gamma}$.

The computed values of α, ζ, ω, γ and ϕ parametrize and reconstruct the signal $y(n)$ in (14). ■

Remark II.2. We compare the developed algorithm against the conventional fast Fourier Transform (FFT) to judge the quality of reconstructing $y(n)$. Figure 2 shows this comparison.

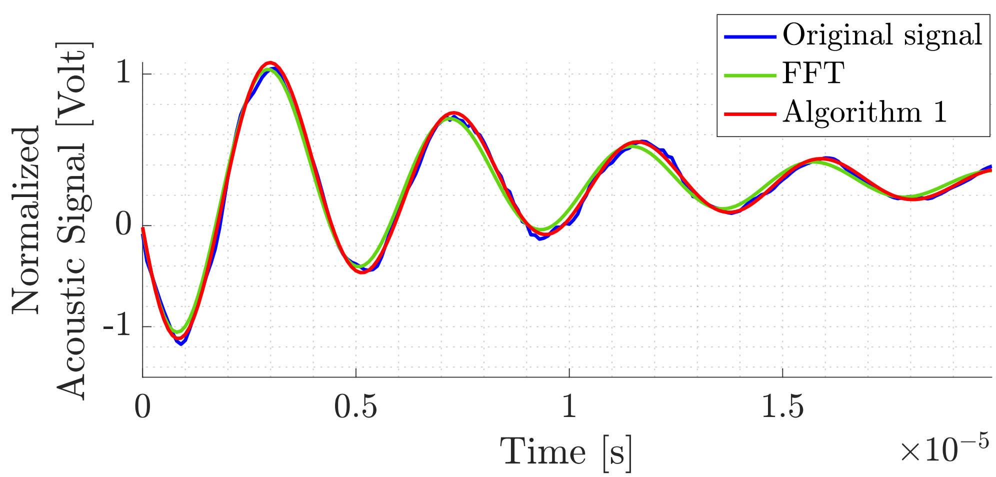

Fig. 2: Comparison of FFT and proposed algorithm to reconstruct $y(n)$.

In Table I, the estimated key parameters are compared. In spite of a little larger computational time, due to increased accuracy, the proposed algorithm is preferred over FFT.

Table I: Key Parameters from the FFT, and Algorithm IV.1

Method	ω (Mrad/s)	α (Volt)	ζ (-)	ϕ (rad)	γ (Volt)	time (s)
FFT	0.1475	166.49	0.0135	-2.8561	-0.8530	0.006
Algorithm IV.1	0.1460	173.26	0.0127	-2.8798	-0.7129	0.008

III. Proof of Theorem VI.1

Proof: Regarding the presented tracking control problem, asymptotic stability is understood with respect to the following non-autonomous error system:

$$\Big(x((k+1)td) - x^r\Big) = \tilde{A}(kt_d)\Big(x(kt_d) - x^r\Big) + \tilde{B}(kt_d)\Big(u^h(kt_d) - u^r(kt_d)\Big). \tag{18}$$

The asymptotic stability of the (18) in closed-loop amounts to verifying whether there exists $\delta > 0$ such that $\lim_{k\to\infty} ||x(kt_d) - x^r|| = 0$ for all initial condition $||x(0) - x^r|| < \delta$ while $u^h(kt_d)$ is applied by solving the MPC problem. To this end, using Lyapunov theory (c.f. [1]), we show that the MPC cost functional $J(k,\cdot,\cdot)$ at instant k, once substituted with unique minimizer $\bar{x}^*(k) := \mathrm{col}(x^*_{1|k}, \cdots x^*_{N|k})$ and $\bar{u}^{h*}_k := \{u^{h*}_{0|k}, \cdots, u^{h*}_{N-1|k}\}$, is a candidate Lyapunov function.

It is now possible to construct an input and state trajectory $\bar{x}^{\mathrm{f}}(k+1), \bar{u}^{\mathrm{f}}(k+1)$ such that the MPC problem at time $k+1$ is feasible (not necessarily optimal) with cost $J^{\mathrm{f}}(k+1, \bar{x}^{\mathrm{f}}(k+1), \bar{u}^{\mathrm{f}}(k+1))$. Here,

$$\bar{x}^{\mathrm{f}}(k+1) = \mathrm{col}\Big(x^*_{2|k}, \cdots x^*_{N|k}, x^{\mathrm{f}}_{N|k+1}\Big),$$

$$\bar{u}^{\mathrm{f}}(k+1) = \mathrm{col}\Big(u^{h*}_{1|k}, \cdots u^{h*}_{N-1|k}, u^{\mathrm{f}}_{N-1|k+1}\Big),$$

where, $x^{\mathrm{f}}_{N|k+1}, u^{\mathrm{f}}_{N-1|k+1}$ are future state and input to be determined by MPC at iteration $k+1$. Similar to the dual mode formulation as proposed in [2], we construct the predicted terminal input at time step $k+1$ as a stabilizing state feedback law for (18). In other words,

$$(x^{\mathrm{f}}_{N|k+1} - x^r) = \Big(\tilde{A}_{N|k} + \tilde{B}_{N|k}K_k\Big)(x^*_{N|k} - x^r).$$

$$u^{\mathrm{f}}_{N-1|k+1} = K_k(x^*_{N|k} - x^r) + u^r_{N|k}.$$

Owing to the convexity and positivity of the objective function, for proving stability, it is sufficient to show that the feasible cost functional is contractive over time samples. In other words,

$$J^{\mathrm{f}}(k+1, \bar{x}^{\mathrm{f}}(k+1), \bar{u}^{\mathrm{f}}(k+1)) < J(k, \bar{x}^*(k), \bar{u}^{h*}(k))$$

Substituting the respective expressions, we obtain

$$\begin{aligned} &J^{\mathrm{f}}(k+1, \bar{x}^{\mathrm{f}}(k+1), \bar{u}^{\mathrm{f}}(k+1)) - J(k, \bar{x}^*(k), \bar{u}^{h*}(k)) \\ &= -||x_{0|k} - x^r||^2_Q - ||u^h_{0|k} - u^r_{0|k}||^2_{R_{0|k}} - ||x^*_{N|k} - x^r||^2_{P_k} \\ &\quad + ||x^*_{N|k} - x^r||^2_Q + ||K_k(x^*_{N|k} - x^r)||^2_{R_{N|k}} + ||(A_{N|k} + B_{N|k}K_k)(x^*_{N|k} - x^r)||^2_{P_k}. \end{aligned} \tag{19}$$

Since the first two terms in the RHS of (19) is negative, we require to satisfy the following inequality for the contraction of the cost functional:

$$(\tilde{A}_{N|k} + \tilde{B}_{N|k}K_k)^\top P_k(\tilde{A}_{N|k} + \tilde{B}_{N|k}K_k) - P_k \preccurlyeq -Q - K_k^\top R_{N|k}K_k, \qquad P_k \succ 0$$

Using changes of variables $X_k = P_k^{-1}$ and $Y_k = K_kP_k^{-1}$ and using the rule of Schur complement we obtain the following LMI:

$$\begin{bmatrix} -X_k & 0 & \tilde{A}_{N|k}X_k + \tilde{B}_{N|k}Y_k & 0 \\ 0 & -R^{-1}_{N|k} & Y_k & 0 \\ (\tilde{A}_{N|k}X_k + \tilde{B}_{N|k}Y_k)^\top & Y_k^\top & -X_k & X_k \\ 0 & 0 & X_k & -Q^{-1} \end{bmatrix} \preccurlyeq 0, \qquad X_k \succ 0.$$

The corresponding control input $u^{\mathrm{f}}_{N-1|k+1} = K_k(x^*_{N|k} - x^r) + u^r_{N|k}$ should also be an admissible control action. In other words, $u^{\mathrm{f}}_{N-1|k+1}$ should satisfy the following constraint:

$$E_{N|k}(K_k(x^*_{N|k} - x^r) + u^r_{N|k}) < b$$

This amounts to the following terminal constraint on $x_{N|k}$:

$$E_{N|k}K_kx_{N|k} < b - u^r_{N|k} + E_{N|k}K_kx^r$$

■

References

[1] F. Blanchini, "Set invariance in control," *Automatica*, vol. 35, no. 11, pp. 1747 – 1767, 1999. [Online]. Available: http://www.sciencedirect.com/science/article/pii/S0005109899001132

[2] M. Sznaier and M. J. Damborg, "Suboptimal control of linear systems with state and control inequality constraints," in *26th IEEE Conference on Decision and Control*, vol. 26, Dec 1987, pp. 761–762.